

Supplementary information

Lactoferrin as an Active Coordination Scaffold for Ruthenium(III)

Tetiana Dyrda-Teraniuk^{*a}, Michalina Ehlert^{a,b}, Kacper Roszak^c, Grzegorz Trykowski^d, Kamil Szpotkowski^e, Łukasz Skowroński^e, Oleksandra Pryshchepa^a, Rudi van Eldik^{b,f}, Katarzyna Mizgalska^{g,h}, Wayne Guida^h, Aleksandra Karolak^g, Riddhi Saindaⁱ, Prafulla K Jhaⁱ, Paweł Pomastowski^{a,b}

^aBioColl team, Centre for Modern Interdisciplinary Technologies, Institute of Advanced Studies, Nicolaus Copernicus University in Toruń, Wileńska 4, 87-100 Toruń, Poland

E-mail: tetiana.dyrda-teraniuk@umk.pl

^bDepartment of Inorganic and Coordination Chemistry, Faculty of Chemistry, Nicolaus Copernicus University in Toruń, Gagarina 7, 87-100 Toruń, Poland

^cDepartment of Immunology, Faculty of Biological and Veterinary Sciences, Nicolaus Copernicus University in Toruń, Lwowska 1, 87-100 Toruń, Poland

^dDepartment of Materials Chemistry, Adsorption and Catalysis, Faculty of Chemistry, Nicolaus Copernicus University in Toruń, Gagarina 7, 87-100 Toruń, Poland

^eDepartment of Surface Physicochemistry, Faculty of Chemical Technology and Engineering, Bydgoszcz University of Science and Technology, Profesora Sylwestra Kaliskiego 7, 85-796 Bydgoszcz, Poland

^fDepartment of Chemistry and Pharmacy, University of Erlangen-Nuremberg, Nikolaus-Fiebiger 10, 91058 Erlangen, Germany

^gDepartment of Machine Learning, Quantitative Science Division, H. Lee Moffitt Cancer Center and Research Institute, 12902 Magnolia Drive, FL 33612, Tampa, USA

^hDepartment of Chemistry, University of South Florida, 4202 East Fowler Avenue, FL 33620, Tampa, USA

ⁱDepartment of Physics, Faculty of Science, The Maharaja Sayajirao University of Baroda, Vadodara, Gujarat 390002, India

- **Isotherm study**

Description of the isotherm models and thermodynamic parameters used to analyze Ru(III) binding to LF

The nature of LF-Ru binding was analyzed by application of two most common isotherm models, such as Langmuir and Freundlich models. The Langmuir model describes the monolayer sorption on the homogeneous sites which are characterized by the equal binding affinity. The model might be expressed as following relationship (1):

$$q_{\text{eq}} = (q_{\text{max}}K_L C_e)/(1 + K_L C_e) \quad (1)$$

where q_{eq} is the amount of bounded Ru(III) per LF [mg/g], q_{max} is the maximum amount of bounded Ru(III) per LF [mg/g], C_e is the equilibrium concentration of Ru(III) [mg/L], K_L is the Langmuir constant [L/mg].

In order to estimate the sorption favorability the dimensionless equilibrium parameter (R_L) might be calculated as follows (2):

$$R_L = 1/(1+K_L C_0) \quad (2)$$

where C_0 is the initial Ru(III) concentration [mg/L]. Based on the R_L value, the sorption process might be defined as: 1) irreversible ($R_L = 0$); 2) favorable ($0 < R_L < 1$); 3) linear ($R_L = 1$), and 4) unfavorable ($R_L > 1$)¹.

In turn, Freundlich model is relevant mathematical model characterizing the multilayer sorption onto heterogeneous surface which might be presented by the following relationship (3):

$$q_{eq} = K_F C_e^{1/n} \quad (3)$$

where K_F is the Freundlich constant [mg/g] and n is the intensity of sorption.

The sorption efficiency of metal binding onto LF was calculated as follows (4):

$$\%E = 100 \times (C_0 - C_{eq}) / C_0 \quad (4)$$

The spontaneity of LF-Ru complex formation was assessed by calculating of the change of Gibbs free energy (ΔG) expressed as (5):

$$\Delta G = -RT \ln K_D \quad (5)$$

where R is the gas constant which is equal to 8.314 J/(K·mol), T is the temperature used for LF-Ru synthesis (310 K), K_D is the distribution coefficient [L/g] which is calculated as the following ratio (6):

$$K_D = q_{eq} / C_{eq} \quad (6)$$

- **Kinetic study**

Description of the kinetic models applied to Ru(III) binding to LF

In order to describe the kinetics of LF-Ru formation, zero-order kinetic model was applied. The following model represent a system where the rate of reaction is not affected by the concentration of reagents (7):

$$C_t = C_0 - k_0 t \quad (7)$$

where C_t is the concentration of Ru(III) at time, C_0 is the initial concentration of Ru(III) at $t = 0$ min [mg/L], k_0 is the zero-order kinetic constant [mg/(L·min)], and t is the time of reaction [min].

Despite it, the application of Weber-Morris model (8) provided the information if the rate of LF-Ru complex formation is limited by intra-particle diffusion step²:

$$q_t = k_{id} t^{0.5} + I \quad (8)$$

where q_t is the sorption capacity [mg/g] of Ru(III) onto LF at time, k_{id} is the intra-particle diffusion rate constant [mg/(g· $\sqrt{\text{min}}$)], I is a constant indicating the thickness of the boundary layer [mg/g].

- **3-D fluorescence spectroscopy analysis**

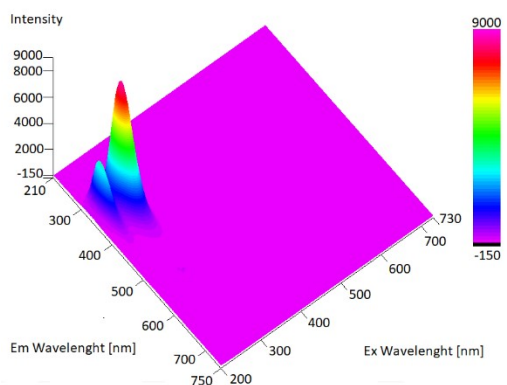


Figure S1. 3D-spectra of bLF dissolved in acetic buffer (pH 4) at the concentration of 100 mg/L.

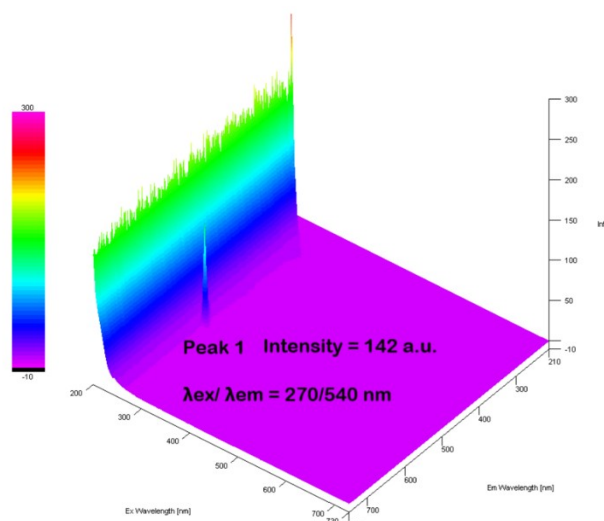


Figure S2. 3D-spectra of empty quartz cuvette.

- **Molecular docking in LF-Ru complex**

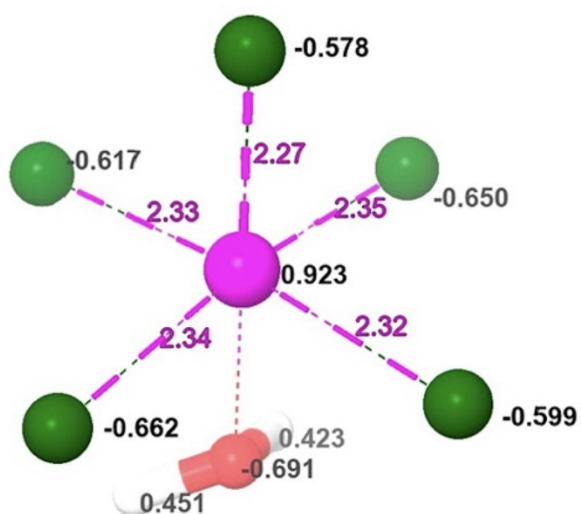


Figure S3. DFT-optimized structure of the $[\text{RuCl}_5(\text{H}_2\text{O})]^{2-}$ complex showing Ru-ligand bond lengths (Å, magenta) and electrostatic potential-derived atomic charges (black).

- **Molecular Dynamics**

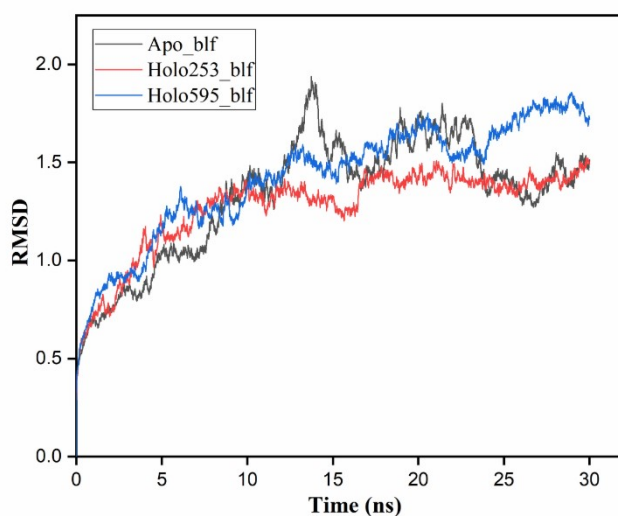


Figure S4. The RMSD of **bLF** systems with and without metal complex.

DFT study

To complement the molecular dynamics (MD) simulations, density functional theory (DFT) calculations were carried out to explore the electronic interactions between the $[\text{RuCl}_5]^{2-}$ complex and representative amino-acid functional groups. Whereas MD describes how the complex approaches and remains associated with the protein over time, the DFT calculations were intended only to provide a simplified picture of how the Ru(III) center may interact chemically with typical donor atoms present on the protein surface. Geometry optimizations were first performed for the isolated metal complex and for individual amino acids. These optimized structures were then used to construct model systems in which the $[\text{RuCl}_5]^{2-}$ species interacts with selected residues suggested by the MD simulations (threonine, cysteine, lysine, and arginine). For each amino acid-complex pair, the candidate configurations were fully relaxed and the lowest-energy structure was taken as the preferred interaction geometry. The resulting optimized structures are shown in Figure S5.

The adsorption energy (E_{ad}) which quantifies the strength of the interaction, was calculated using the following relation ³ (9):

$$E_{\text{ad}} = E_{\text{complex}} - (E_{\text{metal-complex}} + E_{\text{amino-acid}}) \quad (9)$$

where $E_{\text{metal-complex}}$ and $E_{\text{amino-acid}}$ are the total energies of the isolated metal complex and amino acids, whereas E_{complex} is total energy of metal-complex adsorbed amino acids, respectively.

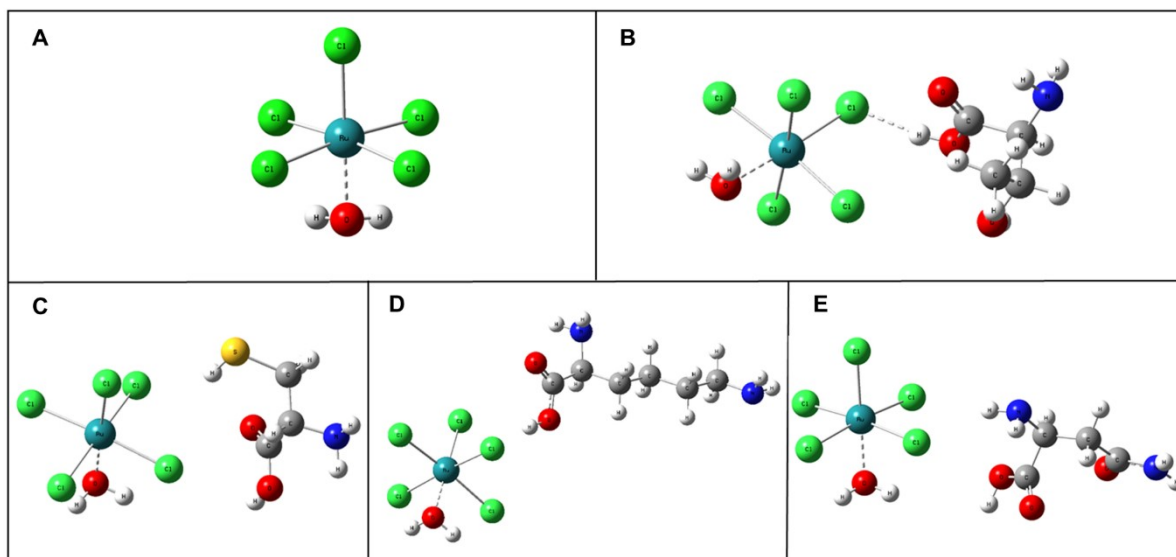


Figure S5. The geometric optimized structure of (A) metal complex, interaction of metal complex with (B) threonine, (C) cysteine, (D) lysine, and (E) arginine.

A more negative adsorption energy implies a stronger and more exergonic interaction, reflecting a greater intrinsic affinity between the metal complex and the isolated amino-acid model⁴. For threonine, the nearest contact occurs between a chlorine atom of the complex and a hydrogen atom from the hydroxyl group at a distance of 2.18 Å, with an adsorption energy of -4.95 eV. Similarly, cysteine, lysine, and arginine display minimum approach distances of 2.63 Å, 3.07 Å, and 2.65 Å with respective adsorption energies of -4.39 eV, -5.03 eV, and -5.33 eV. Among these simplified models, lysine and arginine show the most negative adsorption energies, consistent with comparatively strong electrostatic attraction between their donor groups and the negatively charged metal complex. These values should be interpreted as qualitative donor-affinity trends rather than as direct descriptors of the folded-protein coordination environment.

The interaction trends obtained from the DFT calculations are broadly consistent with the classical MD simulation results, supporting the general donor preferences observed in the trajectory analysis. Minor quantitative differences in adsorption energies and distances can be attributed to methodological differences between the two computational approaches. It should be emphasized that the amino acids were treated as isolated molecules and therefore do not represent the full environment of the folded protein, where steric constraints, neighboring residues, long-range electrostatics, solvent competition, and cooperative effects can substantially influence binding. Hence, the DFT results are not used to define the actual binding site in lactoferrin. Instead, they are interpreted only as qualitative indicators of which donor groups are chemically capable of stabilizing the complex. The specific residue contacts discussed in the main text are derived primarily from the MD trajectory analysis.

In molecular systems, the highest occupied molecular orbital (HOMO) and lowest unoccupied molecular orbital (LUMO) are often used as frontier-orbital descriptors of possible charge redistribution, chemical

reactivity, and redox behavior ^{5,6}. Figure S6 presents the HOMO, LUMO, and Mulliken charge distributions for the isolated metal complex and for the simplified amino-acid adducts.

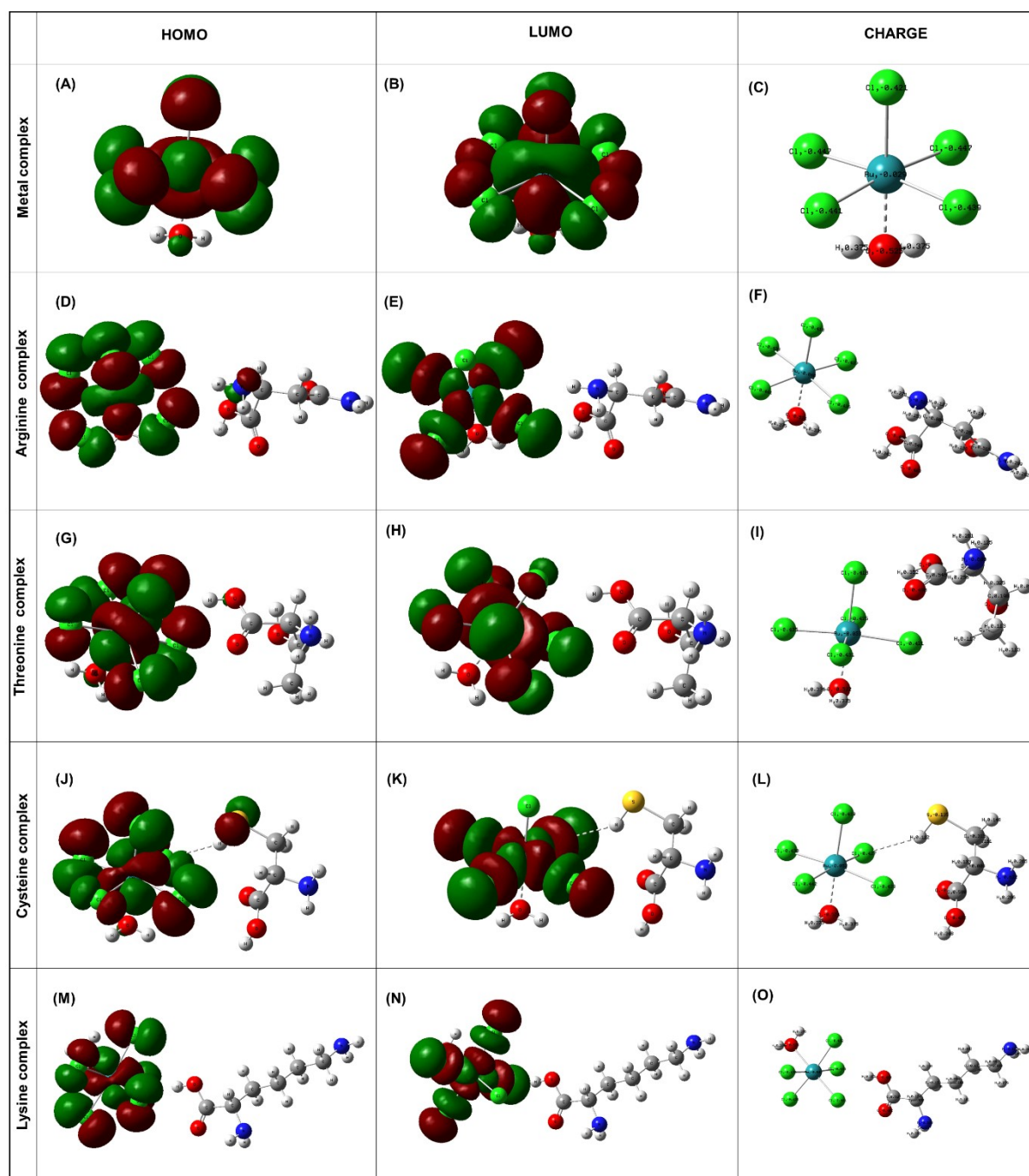


Figure S6. Schematic representation of HOMO, LUMO, and charge redistribution upon interaction of the metal complex with specific amino acid residues of **bLF**.

In these model systems, the orbital distributions change after complex formation, indicating that interaction with N-, O-, and S-donor groups can alter the electronic structure of the Ru species. The largest orbital rearrangements are observed for arginine and cysteine, whereas lysine and threonine show more moderate changes. Mulliken charge analysis likewise indicates residue-dependent redistribution of electron density after adduct formation. These observations are consistent with partial electronic communication between the metal complex and the isolated donor groups. However, because these

calculations were carried out on simplified residue models in the absence of the full protein matrix, solvent competition, and neighboring residues, they should not be interpreted as direct evidence for the extent or direction of charge transfer in folded lactoferrin. Instead, they provide only a qualitative indication that coordination to different donor types can perturb the electronic structure of the Ru complex to different extents.

- **Cytotoxicity of LF-Ru complexes and their impact on cell viability**

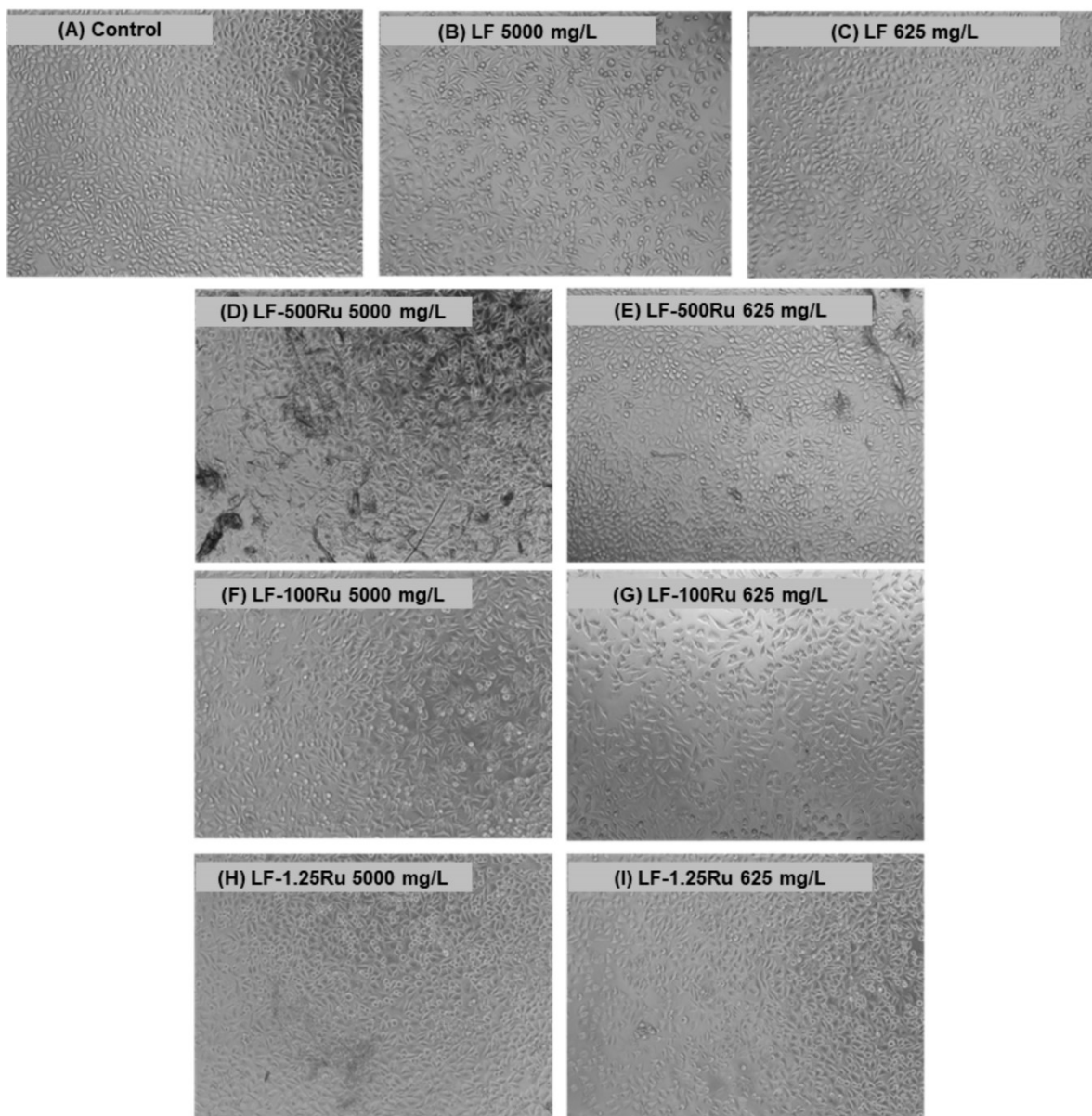


Figure S7. Images of L929 fibroblasts growing on the (A) control, (B-C) LF, (D-E) LF-500Ru, (F-G) LF-100Ru and (H-I) LF-1.25Ru for 2 days. Detailed information regarding the type and concentration of the samples is provided in the figure.

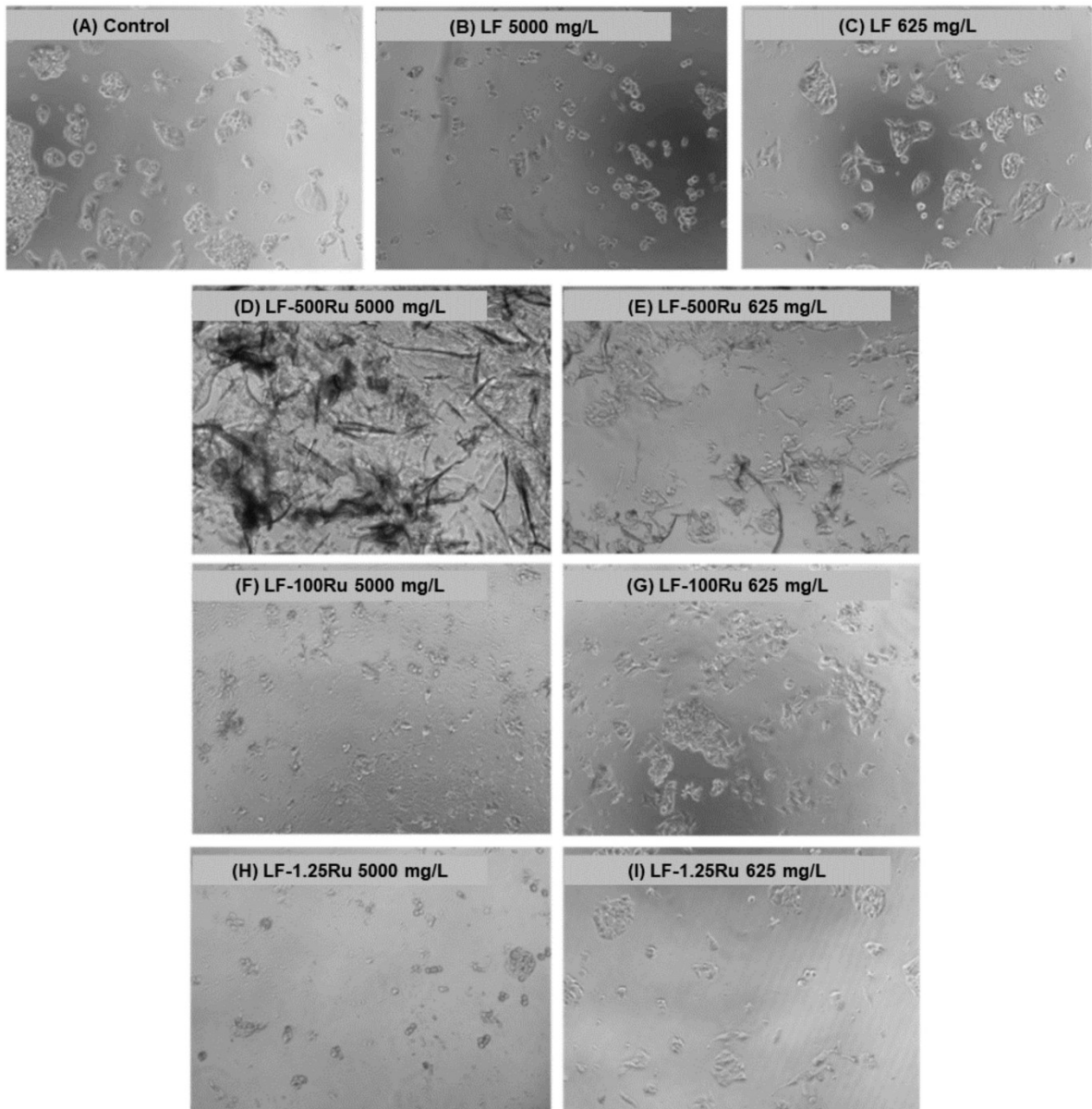


Figure S8. Images of HepG2 growing on the (A) control, (B-C) LF, (D-E) LF-500Ru, (F-G) LF-100Ru and (H-I) LF-1.25Ru for 2 days. Detailed information regarding the type and concentration of the samples is provided in the figure.

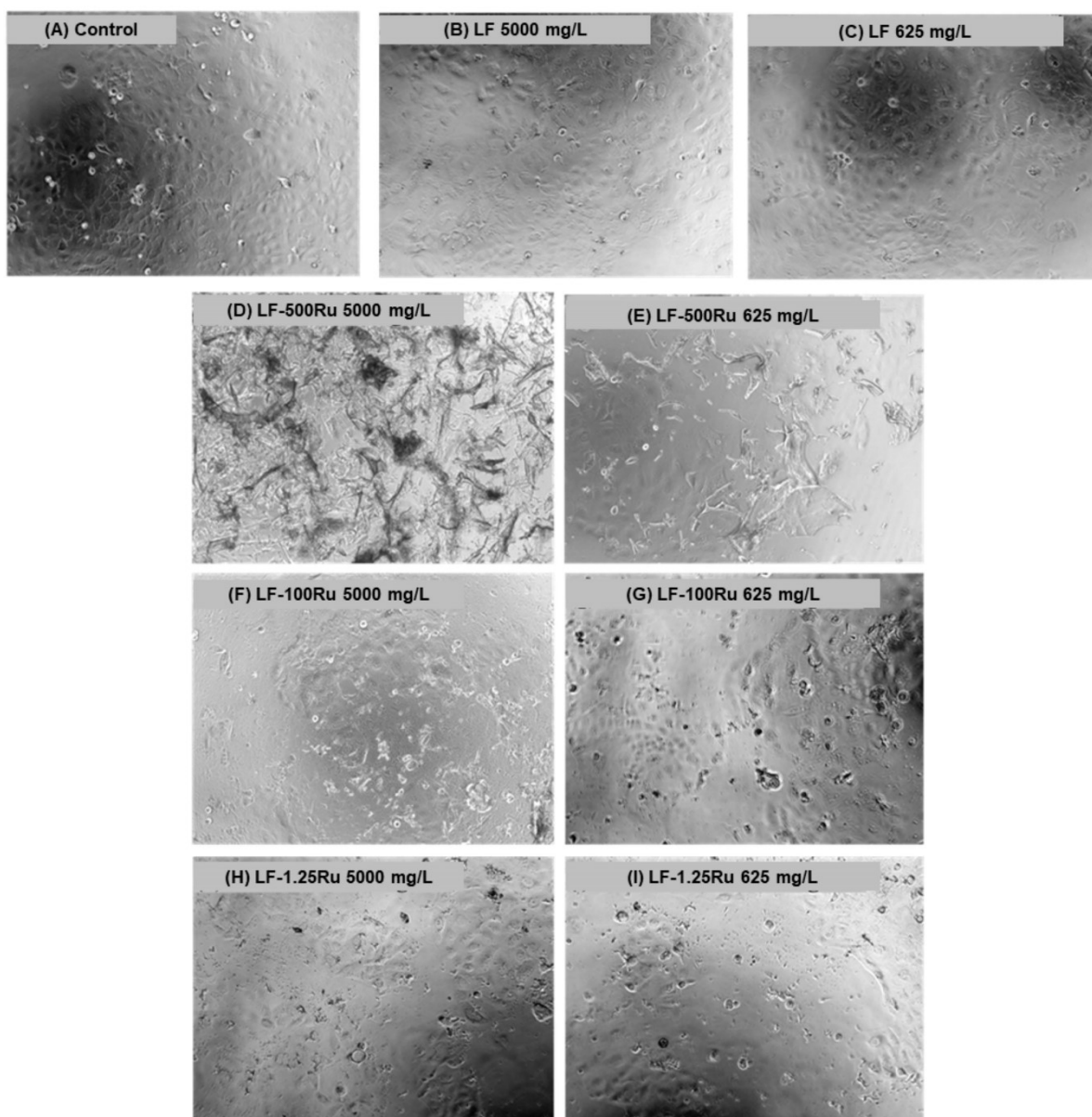


Figure S9. Images of Caco-2 cells growing on the (A) control, (B-C) LF, (D-E) LF-500Ru, (F-G) LF-100Ru and (H-I) LF-1.25Ru for 2 days. Detailed information regarding the type and concentration of the samples is provided in the figure.

Notes and references

- 1 G. Y. Abate, A. N. Alene, A. T. Habte and D. M. Getahun, Adsorptive removal of malachite green dye from aqueous solution onto activated carbon of *Catha edulis* stem as a low cost bio-adsorbent, *Environ. Syst. Res.*, 2020, **9**, 29.
- 2 S. Suresh, V. C. Srivastava and I. M. Mishra, Adsorption of hydroquinone in aqueous solution by granulated activated carbon, *J. Environ. Eng.*, 2011, **137**, 1145–1157.
- 3 R. Sainda, D. Chodvadiya, I. Zgłobicka, K. J. Kurzydłowski and P. K. Jha, The first-principles investigation of sensing and removal applications of nitrobenzene using pPristine and Sc decorated B₉N₉ nanoring, *J. Mol. Liq.*, 2024, **409**, 125389.
- 4 R. Sainda, D. Chodvadiya and P. K. Jha, A DFT study of Mg₉O₉ nanoring for gas sensing and

- removal applications, *J. Mol. Liq.*, 2024, **397**, 124121.
- 5 M. Arjmandi, A. Arjmandi, M. Peyravi and A. K. Pirzaman, First-principles study of adsorption of XCN (X = F, Cl, and Br) on surfaces of polyaniline, *Russ. J. Phys. Chem. A*, 2020, **94**, 2148–2154.
- 6 M. A. Hossain, M. R. Hossain, M. K. Hossain, J. I. Khandaker, F. Ahmed, T. Ferdous and M. A. Hossain, An ab initio study of the B₃₅ boron nanocluster for application as atmospheric gas (NO, NO₂, N₂O, NH₃) sensor, *Chem. Phys. Lett.*, 2020, **754**, 137701.